

This document is confidential and is proprietary to the American Chemical Society and its authors. Do not copy or disclose without written permission. If you have received this item in error, notify the sender and delete all copies.

**Exploring the use of gas chromatography coupled to  
chemical ionization mass spectrometry (GC-CI-MS) for  
stable isotope labeling in metabolomics**

Journal:	<i>Analytical Chemistry</i>
Manuscript ID	Draft
Manuscript Type:	Technical Note
Date Submitted by the Author:	n/a
Complete List of Authors:	<p>Capellades, Jordi; Universitat Rovira i Virgili, Department of Electronic Engineering; Institut d'Investigació Sanitària Pere Virgili (IISPV), Metabolomics Platform; CIBER de Diabetes y Enfermedades Metabólicas Asociadas (CIBERDEM), Instituto de Salud Carlos III</p> <p>Alexandra, Junza; CIBER de Diabetes y Enfermedades Metabólicas Asociadas (CIBERDEM), Instituto de Salud Carlos III</p> <p>Samino, Sara; Universitat Rovira i Virgili, Department of Electronic Engineering; CIBER de Diabetes y Enfermedades Metabólicas Asociadas (CIBERDEM), Instituto de Salud Carlos III</p> <p>Brunner, Julia; Institute for Vascular Biology, Centre for Physiology and Pharmacology, Medical University Vienna; Christian Doppler Laboratory for Arginine Metabolism in Rheumatoid Arthritis and Multiple Sclerosis</p> <p>Schabbauer, Gernot; Institute for Vascular Biology, Centre for Physiology and Pharmacology, Medical University Vienna; Christian Doppler Laboratory for Arginine Metabolism in Rheumatoid Arthritis and Multiple Sclerosis</p> <p>Vinaixa Crevillent, Maria; Universitat Rovira i Virgili, Department of Electronic Engineering; Institut d'Investigació Sanitària Pere Virgili (IISPV), Metabolomics Platform; CIBER de Diabetes y Enfermedades Metabólicas Asociadas (CIBERDEM), Instituto de Salud Carlos III</p> <p>Yanes Torrado, Oscar; Universitat Rovira i Virgili, Department of Electronic Engineering; Institut d'Investigació Sanitària Pere Virgili (IISPV), Metabolomics Platform; Institut d'Investigació Sanitària Pere Virgili (IISPV), Metabolomics Platform</p>

SCHOLARONE™  
Manuscripts

1  
2  
3       1       **Exploring the use of gas chromatography coupled to chemical ionization**  
4       2       **mass spectrometry (GC-CI-MS) for stable isotope labeling in metabolomics**  
5  
6  
7       3

8       4       Jordi Capellades<sup>1,2,3</sup>, Alexandra Junza<sup>2</sup>, Sara Samino<sup>1,2</sup>, Julia S. Brunner<sup>4,5</sup>, Gernot  
9       5       Schabbauer<sup>4,5</sup>, Maria Vinaixa<sup>1,2,3</sup>, Oscar Yanes<sup>1,2,3#</sup>  
10  
11  
12       6

- 13  
14       7       1. Universitat Rovira i Virgili, Department of Electronic Engineering, Tarragona,  
15       8       Spain.  
16  
17       9       2. CIBER de Diabetes y Enfermedades Metabólicas Asociadas (CIBERDEM),  
18       10       Instituto de Salud Carlos III, Madrid, Spain.  
19  
20       11       3. Institut d'Investigació Sanitària Pere Virgili (IISPV), Metabolomics Platform,  
21       12       Reus, Spain.  
22  
23       13       4. Institute for Vascular Biology, Centre for Physiology and Pharmacology,  
24       14       Medical University Vienna, 1090, Vienna, Austria  
25  
26       15       5. Christian Doppler Laboratory for Arginine Metabolism in Rheumatoid Arthritis  
27       16       and Multiple Sclerosis, 1090, Vienna, Austria  
28  
29  
30  
31  
32  
33  
34  
35  
36  
37

38       21       #Corresponding author:

39       22       Oscar Yanes, Ph.D.

40       23       Department of Electronic Engineering

41       24       Universitat Rovira i Virgili

42       25       Avinguda Països Catalans, 26, 43007 Tarragona, Spain

43       26       phone: +34 977759397

44       27       email: [oscar.yanes@urv.cat](mailto:oscar.yanes@urv.cat)  
45  
46  
47  
48  
49  
50  
51  
52  
53  
54  
55  
56  
57  
58  
59  
60

1  
2  
3 29 **Abstract**  
4

5 30 Isotopic labeling experiments have been utterly valuable to monitor the flux of  
6 31 metabolic reactions in biological systems, which is crucial to understand homeostatic  
7 32 alterations with disease. Experimental determination of metabolic fluxes can be inferred  
8 33 from a characteristic rearrangement of stable isotope tracers (e.g.,  $^{13}\text{C}$  or  $^{15}\text{N}$ ) that can  
9 34 be detected by mass spectrometry (MS). Metabolites measured are generally members  
10 35 of well-known metabolic pathways, and most of them can be detected using both gas  
11 36 chromatography (GC)-MS and liquid chromatography (LC)-MS. In here, we show that  
12 37 GC methods coupled to chemical ionization (CI) MS have a clear advantage over  
13 38 alternative methodologies due to GC's superior chromatography separation efficiency  
14 39 and the fact that CI is a soft ionization technique that yields identifiable protonated  
15 40 molecular ion peaks. We tested diverse GC-CI-MS setups, including methane and  
16 41 isobutane reagent gases, triple quadrupole (QqQ) MS in SIM mode or selected ion  
17 42 clusters using optimized narrow-windows (~10 Da) in scan mode, and standard full scan  
18 43 methods using high resolution GC-(q)TOF and GC-Orbitrap systems. Isobutane as  
19 44 reagent gas in combination with both low-resolution (LR) and high-resolution (HR) MS  
20 45 showed the best performance, enabling precise detection of isotopologues in most  
21 46 metabolic intermediates of central carbon metabolism. Finally, with the aim of  
22 47 overcoming manual operations, we developed an R-based tool called isoSCAN that  
23 48 automatically quantifies all isotopologues of intermediate metabolites of glycolysis,  
24 49 TCA cycle, amino acids, pentose phosphate pathway and urea cycle from LRMS and  
25 50 HRMS data.  
26  
27  
28  
29  
30  
31  
32  
33  
34  
35  
36  
37  
38  
39  
40  
41  
42  
43  
44  
45  
46  
47  
48  
49  
50  
51  
52  
53  
54  
55  
56  
57  
58  
59  
60

## 54 Introduction

55 Metabolomics is nowadays a well-established branch of the omics field<sup>1</sup>. The ability to  
56 detect and quantify hundreds of different small organic compounds in complex  
57 biological mixtures makes metabolomics a powerful source of biological information.  
58 Due to the chemical diversity of naturally occurring metabolites, metabolomics is rich  
59 in analytical instrumentation and configurations, with GC-MS and LC-MS/MS being  
60 the most common techniques<sup>2</sup>.

61 GC-MS has been the analytical platform of choice for measuring volatile compounds  
62 for decades<sup>3</sup>. However, with the introduction of chemical derivatization, and the  
63 inherent high-resolution chromatographic separations and low MS background noise,  
64 GC-MS has evolved into a powerful analytical platform to produce compound  
65 abundance data in multiple types of targeted and untargeted metabolomic experiments<sup>4-</sup>  
66 <sup>8</sup>. GC systems are typically coupled to single (GC-sQ) or triple quadrupole mass  
67 spectrometers (GC-QqQ) for targeted metabolomics, while untargeted analyses are  
68 generally performed using time-of-flight (GC-TOF) or Orbitrap (GC-Orbitrap) mass  
69 spectrometers. The most widely used ionization method in GC-MS is electron impact  
70 ionization (EI), a hard ionization strategy that generates highly reproducible and  
71 characteristic fragmentation spectra<sup>3</sup>. However, softer ionization techniques based on  
72 chemical ionization (CI) are alternative methods, where molecular ions of analyzed  
73 compounds are kept (mostly) intact<sup>9</sup>.

74 The determination of relative or absolute metabolite concentrations by GC-MS can also  
75 be used to investigate the rate at which these compounds are being transformed into  
76 other intermediates by metabolic (i.e., enzymatic) activity, a field known as stable-  
77 isotope labeling and fluxomics<sup>10</sup>. Stable isotopes, such as <sup>13</sup>C and <sup>15</sup>N, are used to track  
78 the fate of a labeled nutrient, e.g. <sup>13</sup>C-glucose or <sup>13</sup>C/<sup>15</sup>N-glutamine, being a much safer  
79 and informative alternative to the formerly used radioactive isotopes<sup>11-13</sup>. Metabolites  
80 enriched with stable isotopes maintain the original chemical structure and biochemical  
81 properties, but the different isotopic composition (i.e., isotopologues) causes a shift in  
82 their mass, which is detectable by MS. In this regard, GC-EI MS has become a platform  
83 of choice for stable isotope tracing studies and fluxomics approaches<sup>14-20</sup>. The coverage  
84 of GC-EI MS is comprehensive enough to cover most central carbon metabolism (i.e.,  
85 glycolysis, TCA, amino acids, pentose phosphate pathway) thanks to the use of  
86 chemical derivatization. Several software tools for automated analysis of GC-EI MS  
87 data are available<sup>21-25</sup>, including tools for stable-isotope labeling data analysis<sup>26-32</sup>,

1  
2  
3 88 which must address the inherent difficulty of deconvoluting the intensity of overlapping  
4  
5 89 isotopologues from EI mass spectral fragmentation. Interestingly, the use of GC-CI MS  
6  
7 90 for stable-isotope tracing is largely unexplored<sup>33–37</sup>. In here, we have studied the  
8  
9 91 suitability of GC-CI-MS for stable-isotope tracing using multiple analytical  
10  
11 92 configurations based on low-resolution (LRMS) and high-resolution (HRMS) mass  
12  
13 93 spectrometry. We prove that isobutane is an ideal ionization gas by its ability to yield  
14  
15 94 intact protonated molecular ions, and coupled to cutting-edge high-resolution GC-MS  
16  
17 95 instruments, currently provide the best configuration for isotopologue quantification. In  
18  
19 96 addition, we have developed an R-package called isoSCAN capable of processing GC-  
20  
21 97 CI MS data from LRMS and HRMS stable-isotope labeling studies.  
22

98

## 99 **Methods**

### 100 **Cell cultures**

101 For isotope-labeling experiments, glucose or arginine was replaced with U-13C-glucose  
102 (Cambridge Isotope Labs) or U-13C-Arginine (Sigma Aldrich). Refer to previously  
103 published work for further details on cell culturing<sup>38,39</sup>.

### 104 **Metabolite extraction**

105 Cells were scrapped, collected and frozen. Cell pellets were resuspended with 300  $\mu$ l of  
106 cold methanol/water (8:1, v/v) containing 13C-glycerol (5  $\mu$ l/ml) as internal standard.  
107 Metabolites were extracted with three rounds of liquid N<sub>2</sub> immersion and bath  
108 sonication, followed by 1 h in ice before centrifugation at 22,800  $\times$  g (10 min at 4 °C).  
109 The supernatant was set aside for derivatization in a new tube.

### 110 **Derivatization**

111 Samples were dried under a stream of N<sub>2</sub> gas and lyophilized before chemical  
112 derivatization with 40  $\mu$ l of methoxyamine in pyridine (30  $\mu$ g/ml) for 45 min at 60 °C.  
113 Samples were also silylated using 25  $\mu$ l of *N*-methyl-*N*-trimethylsilyltrifluoroacetamide  
114 with 1% trimethylchlorosilane (Thermo Fisher Scientific) for 30 min at 60 °C to  
115 increase volatility of metabolites.

### 116 **LRMS acquisition**

117 A 7890A GC system coupled to a 7000 QqQ mass spectrometer (Agilent Technologies)  
118 was used for isotopologue determination for the low-resolution datasets using SIM and  
119 NS acquisition modes. Derivatized samples were injected (1  $\mu$ l) in the gas  
120 chromatograph system with a split inlet equipped with a J&W Scientific HP-5ms  
121 stationary phase column (30 m  $\times$  0.25 mm i.d., 0.1  $\mu$ m film, Agilent Technologies). The

1  
2  
3 122 injector split ratio was adjusted to 1:5. Helium was used as a carrier gas at a flow rate of  
4  
5 123 1 mL/min in constant flow mode. In the method to quantify TCA metabolites, the oven  
6  
7 124 temperature was programmed to sit at 70 °C for 1 min and afterwards increase at  
8  
9 125 10 °C/min to 325 °C. On the other hand, in the polyamines method (Supplementary  
10  
11 126 table 1) the temperature gradient was the following: from 70 to 150 °C at a heating rate  
12  
127 of 5 °C/min, from 150 to 250 °C at 10 °C/min and from 250 to 325 °C at 50 °C/min.  
13  
128 Metabolites were ionized using positive chemical ionization (CI) with isobutane or  
14  
15 129 methane as reagent gas.

### 16 17 130 **HRMS acquisition**

18  
19 131 A 7890B GC system coupled to a 7250 QTOF mass spectrometer (Agilent  
20  
21 132 Technologies) was used. Derivatized samples were injected (1 µl) in the gas  
22  
23 133 chromatograph system equipped with an Agilent 19091S-433UI HP5-ms Ultra Inert  
24  
25 134 stationary phase column (30 m x 0.25 mm x 0.25 µm, Agilent Technologies). Helium  
26  
27 135 was used as a carrier gas at a flow rate of 1.5 mL/min in constant flow mode. The  
28  
29 136 temperature gradient used was: from 70 to 190 °C at a heating rate of 11 °C/min, and  
30  
31 137 from 190 to 325 °C at 21°C/min, finally holding for 4 min. Metabolites were ionized  
32  
33 138 using positive chemical ionization (CI) with isobutane as reagent gas. Mass spectral  
34  
35 139 data were acquired in full scan mode (110 – 800 m/z) at and an acquisition rate of 3 Hz.  
36  
37 140 A TRACE 1300 Series GC coupled to an Orbitrap Q Exactive mass spectrometer  
38  
39 141 (Thermo Scientific) was used for isotopologue determination. Derivatized samples were  
40  
41 142 injected (1 µl) in the gas chromatograph system with a split inlet 1:5 equipped with a  
42  
43 143 TraceGOLD-5MS stationary phase column (30 m x 0.25 mm x 0.25µm film, Thermo  
44  
45 144 Scientific). Helium was used as a carrier gas at a flow rate of 1.5 mL/min.  
46  
47 145 The temperature gradient used was: from 70 to 190 °C at a heating rate of 11 °C/min,  
48  
49 146 and from 190 to 325 °C at 21°C/min, finally holding for 2.7 min. Mass spectral data  
50  
51 147 were acquired in full scan mode (150 – 750 m/z) and the AGC target was set to 1  
52  
53 148 million (1x10<sup>6</sup>). The analyzer resolution settings were 60,000 at 200 m/z. Metabolites  
54  
55 149 were ionized using positive chemical ionization (CI) with isobutane as reagent gas, also  
56  
57 150 low-energy (15eV) and high-energy (70eV) electron impact (EI) ionization was used  
58  
59 151 (Supplementary Figure 1).  
60

## 154 **Results**

### 155 **Comparing Electron Ionization (EI) with Chemical Ionization (CI) for stable** 156 **isotope labeling**

157 In order to optimize the detection of isotopologues using GC-MS, we first compared the  
158 performance of the most commonly used ionization sources in GC-MS: EI and CI.  
159 Furthermore, we tested two different reagent gases for CI, namely methane and  
160 isobutane. Taking lactate as a reference metabolite in a complex biological mixture such  
161 as  $^{13}\text{C}$ -U-glucose labeled and non-labeled cell cultures, we found that CI with  
162 isobutane yielded most suitable spectra to detect isotopic enrichments in comparison  
163 with EI (Figure 1A). Notably, the use of isobutane as reagent gas produced mass spectra  
164 in which the abundance of a metabolite is typically concentrated in its  $[\text{M}+\text{H}]^+$  isotopic  
165 envelop, facilitating the detection of isotopic enrichment, unlike methane gas that  
166 induced unwanted fragmentation of the  $[\text{M}+\text{H}]^+$  ion (Figure 1B). This observation also  
167 applied to all intermediates of the glycolytic pathway and TCA cycle, where the  
168  $[\text{M}+\text{H}]^+$  ion was, on average, >5-fold more intense using isobutane than methane  
169 (Figure 1C). In contrast, EI at 70 eV is a hard ionization technique causing extensive  
170 fragmentation of compound structures in both non-labeled and labeled samples. This  
171 complicates the process of determining the amount of isotope labeling because the  
172 isotopic enrichment is scattered throughout multiple fragments. Similarly, low-energy  
173 EI at 15 eV<sup>31</sup> also produced greater fragmentation of the molecular ion than CI-  
174 isobutane (Suppl. Figure S1).

175 Finally, we show that CI-isobutane can ionize efficiently most relevant metabolites  
176 found in central carbon metabolism pathways, including intermediates of glycolysis,  
177 TCA cycle, pentose phosphate pathway, amino acids, urea cycle and polyamines  
178 (Supplementary Table1). In summary, CI-isobutane resulted in a broad coverage of  
179 metabolites in addition to greater signal intensity of the  $[\text{M}+\text{H}]^+$  molecular ion for all  
180 metabolites tested.

181

### 182 **Optimizing data acquisition modes in GC-CI MS for stable isotope labeling**

183 The collection of mass analyzers used in hyphenated mass-spectrometry is quite broad  
184 nowadays. To test the capabilities of GC-CI MS for stable isotope labeling, we  
185 compared the sensitivity, selectivity and isotope ratio fidelity of different mass  
186 analyzers and data acquisition modes. In particular, we used a low-mass resolution  
187 configuration based on GC-CI triple quadrupole MS, and two high-mass resolution

1  
2  
3 188 configurations based on GC-CI qTOF MS and GC-CI qOrbitrap MS to analyze the  
4  
5 189 same labeled and non-labeled complex biological mixtures. In the case of the  
6  
7 190 quadrupole configuration, we explored two acquisition modes to find the most sensitive  
8  
9 191 and selective for isotopologue analysis: selected ion monitoring (SIM) and narrow scan  
10 192 (NS) acquisition.

11 193 SIM acquisition method was set to monitor single ions, that is, every isotopologue based  
12 194 on the number of carbons in each metabolite. In contrast, NS acquisition method was set  
13 195 to register a cluster of ions that covers the full isotopic envelope (typically 8-10 Da) of  
14 196 the derivatized metabolite, e.g. in the case of lactate-2TMS ( $m/z$  235) the quadrupole  
15 197 was set to scan a mass range from  $m/z$  232 to 240. Despite the greater signal intensity of  
16 198 NS for all metabolites tested, SIM yielded better signal-to-noise ratios (SNR), likely due  
17 199 to its greater ion selectivity (Figure 2A). The isotope ratio fidelity of NS and SIM,  
20 200 calculated as the relative deviation to the theoretical isotopic ratio, was similar in both  
21 201 acquisition methods, showing a median value of 5% from a total of 14 metabolites  
22 202 detected in 9 cell culture replicates (Figure 2B).

23 203 Next, we compared the sensitivity, selectivity and isotope ratio fidelity of two high-  
24 204 mass resolution instruments: a GC-qOrbitrap mass analyzer acquiring in full scan mode  
25 205 at 60.000 resolution (at  $m/z$  200) and a GC-qTOF mass analyzer acquiring in full scan  
26 206 mode at  $\sim$ 16.000 resolution. The median deviation of isotopologue abundances in  
27 207 relation to theoretical natural abundances was 19% for GC-CI qOrbitrap MS and 26%  
28 208 for GC-CI qTOF MS, yet only the Orbitrap mass analyzer was capable of clearly  
29 209 resolving natural isotopes of silicon ( $^{29}\text{Si}$  and  $^{30}\text{Si}$  from the trimethylsilyl  
30 210 derivatization) from carbon, while in the case of the TOF mass analyzer silicon and  
31 211 carbon isotopes were practically indistinguishable and thus were summed up (Figure  
32 212 2C). As expected, the Orbitrap showed a better mass accuracy ( $<1.5$  ppm) compared to  
33 213 the TOF mass analyzer ( $<8$  ppm).

34 214 Interestingly, when the quadrupole of the GC qOrbitrap was set to filter the same cluster  
35 215 of ions that covers the full isotopic envelope of the derivatized metabolites as in NS,  
36 216 with the aim of reducing the ion population in the Orbitrap mass analyzer, we did not  
37 217 observe an increase in sensitivity in comparison with full scan acquisition (data not  
38 218 shown). As expected, both high-mass resolution instruments have the additional  
39 219 advantage that are more selective than low-mass resolution methods SIM and NS,  
40 220 because the former can distinguish artifacts (such as background noise) or compounds  
41 221 that could interfere with the detection of the isotopologues of interest. This is

1  
2  
3 222 particularly important when detecting labeled isotopologues of low abundant  
4 223 compounds in biological samples (see aconitate 3TMS and dihydroxy-acetone  
5 224 phosphate 3TMS+MA in Figure 2D).

6  
7  
8 225 In summary, our results demonstrate that GC CI-isobutane is an optimal configuration  
9 226 for the detection of isotopologues, and the latest generation of high-mass resolution GC-  
10 227 MS instruments in full scan mode have similar sensitivity than quadrupole-based mass  
11  
12 228 analyzers. In counterpoint, the isotope ratio fidelity is superior in LRMS than HRMS.  
13  
14  
15 229

### 16 17 230 **isoSCAN: an R package to process GC-CI-MS data from low-mass and high-mass** 18 231 **resolution acquisition methods**

19  
20 232 To extend high throughput capabilities of GC-CI-MS for stable isotope labeling studies,  
21 233 we have developed *isoSCAN*, an open-source R-based computational tool  
22 234 (<https://github.com/jcapelladesto/isoSCAN>) that encloses a complete workflow to  
23 235 perform high-throughput compound-driven isotopologue quantification in GC-MS data,  
24 236 either from high- or low-mass resolution instrumentation. The performance of *isoSCAN*  
25 237 has been assayed in several stable isotope labeling studies so far<sup>38-43</sup>.

26  
27 238 *isoSCAN* computational workflow is summarized in Figure 3A. *isoSCAN* requires GC-  
28 239 MS files in open standard formats (mz(X)ML) as input data, and a list of compounds to  
29 240 target with their associated molecular formulas, monoisotopic mass values, and  
30 241 estimated retention times (Supplementary Table1). The software processes each file  
31 242 independently, targeting each singular isotopologue peak of every targeted compound  
32 243 within a specified retention time range through local maxima detection. This process  
33 244 differs slightly from low to high mass resolution data. In the case of low-resolution  
34 245 instruments, *autoQ* computes the isotopologue mass by adding the corresponding  
35 246 enrichment isotope mass difference (i.e., 1.003355 for <sup>13</sup>C) as many times as the  
36 247 maximum number of atoms present in the non-derivatized molecular formula (i.e., up to  
37 248 six times in the case of glucose (C<sub>6</sub>H<sub>12</sub>O<sub>6</sub>)). To perform on low-resolution data, such  
38 249 data must be in profile mode, as this facilitates the elucidation of spectral peaks. For  
39 250 high-resolution data, isotopologue quantification supports centroided data. We observed  
40 251 that isotopologue mass calculation need to be refined as mass spectral data may include  
41 252 other isotopic peaks from Si, N or O that are relatively less intense but still must be  
42 253 considered for accurate quantification. Therefore, *autoQ* makes use of *enviPat*<sup>44</sup>  
43 254 functionalities to calculate and merge the theoretical isotopic distribution given an  
44 255 estimated mass resolution. Each different isotopologue m/z is then searched separately  
45  
46  
47  
48  
49  
50  
51  
52  
53  
54  
55  
56  
57  
58  
59  
60

1  
2  
3 256 by minimizing the cumulative relative mass error (ppm) in order to avoid  
4  
5 257 misassignments. Afterwards, isotopologue abundances are added by considering the  
6  
7 258 number of labeled atoms to which each isotopologue corresponds (see Figure 3B for an  
8  
9 259 example in the case of isotopologues M+0 to M+3 of lactate 2TMS).

10 260

## 11 261 **Discussion and conclusions**

12 262 MS is currently the preferred analytical technique used for measuring stable-isotope  
13 263 labeling of metabolites. In this regard, GC-MS is characterized by low cost and  
14 264 relatively simple maintenance, which makes it more affordable than LC-MS equipment  
15 265 by many individual laboratories. A desirable scenario of stable-isotope labeling is to  
16 266 measure isotopologue distributions in intact metabolites, however, the inherent  
17 267 fragmentation of EI (the most widespread used ionization source in GC-MS) cause  
18 268 scattered isotope patterns. To minimize fragmentation, different analytical strategies  
19 269 have been implemented, including chemical derivatization with N-methyl N-(*tert*-  
20 270 butylsilyl)trifluoroacetamide (MTBSTFA)<sup>15</sup>, EI ionization at 15 eV <sup>31</sup> or the use of  
21 271 chemical ionization<sup>37</sup>. The latter has been traditionally implemented using methane as  
22 272 reagent gas<sup>31</sup>, however, isobutane produces superior intact analyte signal abundance to  
23 273 methane<sup>45</sup>, resulting also in a predominant protonated adduct ion and less fragmentation.  
24 274 Here we have used this previous knowledge to demonstrate that CI-isobutane  
25 275 outperforms CI-methane, EI at 70eV and EI at 15eV for isotopologue analysis by GC-  
26 276 MS. We have also shown that the metabolic coverage of CI-isobutane allows analysis of  
27 277 most relevant metabolites in central carbon metabolism with good ionization efficiency,  
28 278 including intermediates of glycolysis, TCA cycle, pentose phosphate pathway, amino  
29 279 acids, urea cycle and polyamines. In addition, we have benefited from this better suited  
30 280 ionization source to explore different acquisition modes from the most common mass  
31 281 analyzers in metabolomics: time-of-flight (TOF), orbitrap, and quadrupole.  
32 282 Quadrupoles act as low-resolution mass filters and can be placed in series (e.g., triple  
33 283 quadrupoles) to measure only a predefined subset of ions, offering in principle the best  
34 284 sensitivity for measuring a single metabolite. Our results showed that monitoring every  
35 285 isotopologue by selected ion monitoring (SIM) or opening the quadrupole 8-10 Da to  
36 286 scan the whole cluster of isotopologues of a metabolite, yielded similar results with  
37 287 regard to sensitivity; that is to say, despite the better signal-to-noise ratios of SIM or the  
38 288 higher absolute intensity counts of the narrow scan (NS) acquisition, the same  
39 289 isotopologues were detected for low abundant metabolites. Remarkably, our results also

1  
2  
3 290 indicate that, despite LRMS shows higher isotopic fidelity than HRMS, cutting-edge  
4  
5 291 high-resolution GC-MS instruments improve detection of certain isotopologues in low  
6  
7 292 abundant compounds. Barely distinguishable isotopologues in SIM and/or NS showed a  
8  
9 293 considerably higher and selective response in full scan acquisition mode with HRMS  
10  
11 294 instruments such as the GC Orbitrap, probably as a result of increased capacity to  
12  
13 295 distinguish m/z interferences.

14 296 Finally, we have developed a versatile open-source software that can automatically  
15  
16 297 process low- and high-resolution isotopic labeling data produced with GC CI-isobutane  
17  
18 298 coupled to quadrupole, TOF and orbitrap instruments.

19 299

20  
21 300

### 22 23 301 **Acknowledgements**

24  
25 302 OY thanks the following bodies for funding: Ministerio de Economía y Competitividad  
26  
27 303 (MINECO) (BFU2014-57466-P) and the Spanish Biomedical Research Centre  
28  
29 304 in Diabetes and Associated Metabolic Disorders (CIBERDEM), an initiative of Instituto  
30  
31 305 de Investigación Carlos III (ISCIII).

32  
33 306

34  
35 307

36  
37 308

38  
39 309

40  
41 310

42  
43 311

44  
45 312

46  
47 313

48  
49 314

50  
51 315

52  
53 316

54  
55 317

56  
57 318

319

320 **References**

- 321 (1) Patti, G. J.; Yanes, O.; Siuzdak, G. Innovation: Metabolomics: The Apogee of the  
322 Omics Trilogy. *Nat. Rev. Mol. Cell Biol.* **2012**, *13* (4), 263–269.  
323 <https://doi.org/10.1038/nrm3314>.
- 324 (2) Vinaixa, M.; Schymanski, E. L.; Neumann, S.; Navarro, M.; Salek, R. M.; Yanes,  
325 O. Mass Spectral Databases for LC/MS- and GC/MS-Based Metabolomics: State  
326 of the Field and Future Prospects. *TrAC Trends Anal. Chem.* **2016**, *78*, 23–35.  
327 <https://doi.org/10.1016/J.TRAC.2015.09.005>.
- 328 (3) Fiehn, O. Metabolomics by Gas Chromatography-Mass Spectrometry: Combined  
329 Targeted and Untargeted Profiling. *Curr. Protoc. Mol. Biol.* **2016**, *114*, 30.4.1-  
330 30.4.32. <https://doi.org/10.1002/0471142727.mb3004s114>.
- 331 (4) Dunn, W. B.; Broadhurst, D. I.; Atherton, H. J.; Goodacre, R.; Griffin, J. L.  
332 Systems Level Studies of Mammalian Metabolomes: The Roles of Mass  
333 Spectrometry and Nuclear Magnetic Resonance Spectroscopy. *Chem. Soc. Rev.*  
334 **2011**, *40* (1), 387–426. <https://doi.org/10.1039/b906712b>.
- 335 (5) Krilaviciute, A.; Heiss, J. A.; Leja, M.; Kupcinskas, J.; Haick, H.; Brenner, H.  
336 Detection of Cancer through Exhaled Breath: A Systematic Review. *Oncotarget*  
337 **2015**, *6* (36), 38643–38657. <https://doi.org/10.18632/oncotarget.5938>.
- 338 (6) Psychogios, N.; Hau, D. D.; Peng, J.; Guo, A. C.; Mandal, R.; Bouatra, S.;  
339 Sinelnikov, I.; Krishnamurthy, R.; Eisner, R.; Gautam, B.; Young, N.; Xia, J.;  
340 Knox, C.; Dong, E.; Huang, P.; Hollander, Z.; Pedersen, T. L.; Smith, S. R.;  
341 Bamforth, F.; Greiner, R.; McManus, B.; Newman, J. W.; Goodfriend, T.;  
342 Wishart, D. S. The Human Serum Metabolome. *PLoS One* **2011**, *6* (2), e16957.  
343 <https://doi.org/10.1371/journal.pone.0016957>.
- 344 (7) Bouatra, S.; Aziat, F.; Mandal, R.; Guo, A. C.; Wilson, M. R.; Knox, C.;  
345 Bjorn Dahl, T. C.; Krishnamurthy, R.; Saleem, F.; Liu, P.; Dame, Z. T.; Poelzer,  
346 J.; Huynh, J.; Yallou, F. S.; Psychogios, N.; Dong, E.; Bogumil, R.; Roehring, C.;  
347 Wishart, D. S. The Human Urine Metabolome. *PLoS One* **2013**, *8* (9), e73076.  
348 <https://doi.org/10.1371/journal.pone.0073076>.
- 349 (8) Sreekumar, A.; Poisson, L. M.; Rajendiran, T. M.; Khan, A. P.; Cao, Q.; Yu, J.;  
350 Laxman, B.; Mehra, R.; Lonigro, R. J.; Li, Y.; Nyati, M. K.; Ahsan, A.; Kalyana-  
351 Sundaram, S.; Han, B.; Cao, X.; Byun, J.; Omenn, G. S.; Ghosh, D.; Pennathur,

- 1  
2  
3 352 S.; Alexander, D. C.; Berger, A.; Shuster, J. R.; Wei, J. T.; Varambally, S.;  
4 353 Beecher, C.; Chinnaiyan, A. M. Metabolomic Profiles Delineate Potential Role  
5 354 for Sarcosine in Prostate Cancer Progression. *Nature* **2009**, *457* (7231), 910–914.  
6 355 <https://doi.org/10.1038/nature07762>.  
7  
8  
9  
10 356 (9) Kopka, J.; Schauer, N.; Krueger, S.; Birkemeyer, C.; Usadel, B.; Bergmuller, E.;  
11 357 Dormann, P.; Weckwerth, W.; Gibon, Y.; Stitt, M.; Willmitzer, L.; Fernie, A. R.;  
12 358 Steinhauser, D. GMD@CSB.DB: The Golm Metabolome Database.  
13 359 *Bioinformatics* **2005**, *21* (8), 1635–1638.  
14 360 <https://doi.org/10.1093/bioinformatics/bti236>.  
15  
16  
17  
18 361 (10) Jang, C.; Chen, L.; Rabinowitz, J. D. Metabolomics and Isotope Tracing. *Cell*  
19 362 **2018**, *173* (4), 822–837. <https://doi.org/10.1016/j.cell.2018.03.055>.  
20  
21  
22 363 (11) Gibbs, M.; Kandler, O. ASYMMETRIC DISTRIBUTION OF C IN SUGARS  
23 364 FORMED DURING PHOTOSYNTHESIS. *Proc. Natl. Acad. Sci. U. S. A.* **1957**,  
24 365 *43* (6), 446–451. <https://doi.org/10.1073/pnas.43.6.446>.  
25  
26  
27 366 (12) Katz, J. The Application of Isotopes to the Study of Lactate Metabolism. *Med.*  
28 367 *Sci. Sports Exerc.* **1986**, *18* (3), 353–359. [https://doi.org/10.1249/00005768-](https://doi.org/10.1249/00005768-198606000-00018)  
29 368 [198606000-00018](https://doi.org/10.1249/00005768-198606000-00018).  
30  
31  
32 369 (13) Batista Silva, W.; Daloso, D. M.; Fernie, A. R.; Nunes-Nesi, A.; Araújo, W. L.  
33 370 Can Stable Isotope Mass Spectrometry Replace radiolabeled Approaches in  
34 371 Metabolic Studies? *Plant Sci.* **2016**, *249*, 59–69.  
35 372 <https://doi.org/10.1016/j.plantsci.2016.05.011>.  
36  
37  
38 373 (14) Zamboni, N.; Fendt, S.-M.; Rühl, M.; Sauer, U. <sup>13</sup>C-Based Metabolic Flux  
39 374 Analysis. *Nat. Protoc.* **2009**, *4* (6), 878–892.  
40 375 <https://doi.org/10.1038/nprot.2009.58>.  
41  
42  
43 376 (15) Higashi, R. M.; Fan, T. W.-M.; Lorkiewicz, P. K.; Moseley, H. N. B.; Lane, A.  
44 377 N. Stable Isotope-Labeled Tracers for Metabolic Pathway Elucidation by GC-MS  
45 378 and FT-MS. In *Methods in molecular biology (Clifton, N.J.)*; 2014; Vol. 1198, pp  
46 379 147–167. [https://doi.org/10.1007/978-1-4939-1258-2\\_11](https://doi.org/10.1007/978-1-4939-1258-2_11).  
47  
48  
49 380 (16) Sauer, U. Metabolic Networks in Motion: <sup>13</sup>C-Based Flux Analysis. *Mol. Syst.*  
50 381 *Biol.* **2006**, *2*, 62. <https://doi.org/10.1038/msb4100109>.  
51  
52  
53 382 (17) Schlotterbeck, G.; Ross, A.; Dieterle, F.; Senn, H. Metabolic Profiling  
54 383 Technologies for Biomarker Discovery in Biomedicine and Drug Development.  
55 384 *Pharmacogenomics* **2006**, *7* (7), 1055–1075.  
56 385 <https://doi.org/10.2217/14622416.7.7.1055>.  
57  
58  
59  
60

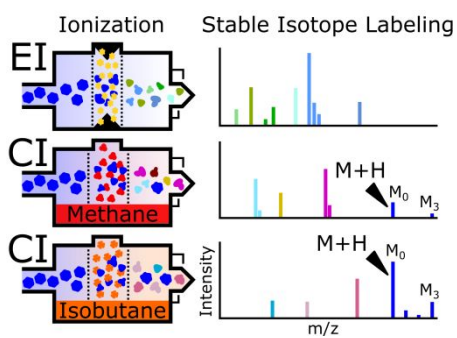
- 1  
2  
3 386 (18) Zamboni, N. Toward Metabolome-Based <sup>13</sup>C Flux Analysis: A Universal Tool  
4 for Measuring in Vivo Metabolic Activity; Springer, Berlin, Heidelberg, 2007; pp  
5 387  
6 388 129–157. [https://doi.org/10.1007/4735\\_2007\\_0220](https://doi.org/10.1007/4735_2007_0220).
- 7  
8 389 (19) Wiechert, W.; Möllney, M.; Petersen, S.; de Graaf, A. A. A Universal  
9 Framework for <sup>13</sup>C Metabolic Flux Analysis. *Metab. Eng.* **2001**, *3* (3), 265–283.  
10 390  
11 391 <https://doi.org/10.1006/mben.2001.0188>.
- 12  
13 392 (20) Jang, C.; Chen, L.; Rabinowitz, J. D. Metabolomics and Isotope Tracing. *Cell*  
14 **2018**, *173* (4), 822–837. <https://doi.org/10.1016/j.cell.2018.03.055>.
- 15 393  
16 394 (21) Bunk, B.; Kucklick, M.; Jonas, R.; Münch, R.; Schobert, M.; Jahn, D.; Hiller, K.  
17 MetaQuant: A Tool for the Automatic Quantification of GC/MS-Based  
18 395  
19 396 Metabolome Data. *Bioinformatics* **2006**, *22* (23), 2962–2965.  
20 397  
21 397 <https://doi.org/10.1093/bioinformatics/btl526>.
- 22  
23 398 (22) Lei, Z.; Li, H.; Chang, J.; Zhao, P. X.; Sumner, L. W. MET-IDEA Version 2.06;  
24 Improved Efficiency and Additional Functions for Mass Spectrometry-Based  
25 399  
26 400 Metabolomics Data Processing. *Metabolomics* **2012**, *8* (S1), 105–110.  
27 401  
28 401 <https://doi.org/10.1007/s11306-012-0397-5>.
- 29  
30 402 (23) Hiller, K.; Hangebrauk, J.; Jäger, C.; Spura, J.; Schreiber, K.; Schomburg, D.  
31 MetaboliteDetector: Comprehensive Analysis Tool for Targeted and Nontargeted  
32 403  
33 404 GC/MS Based Metabolome Analysis. *Anal. Chem.* **2009**, *81* (9), 3429–3439.  
34 405  
35 405 <https://doi.org/10.1021/ac802689c>.
- 36  
37 406 (24) Domingo-Almenara, X.; Brezmes, J.; Vinaixa, M.; Samino, S.; Ramirez, N.;  
38 407  
39 407 Ramon-Krauel, M.; Lerin, C.; Díaz, M.; Ibáñez, L.; Correig, X.; Perera-Lluna,  
40 408  
41 408 A.; Yanes, O. ERah: A Computational Tool Integrating Spectral Deconvolution  
42 409  
43 409 and Alignment with Quantification and Identification of Metabolites in GC/MS-  
44 410  
45 410 Based Metabolomics. *Anal. Chem.* **2016**, *88* (19), 9821–9829.  
46 411  
47 411 <https://doi.org/10.1021/acs.analchem.6b02927>.
- 48 412 (25) Ni, Y.; Su, M.; Qiu, Y.; Jia, W.; Du, X. ADAP-GC 3.0: Improved Peak Detection  
49 413  
50 413 and Deconvolution of Co-Eluting Metabolites from GC/TOF-MS Data for  
51 414  
52 414 Metabolomics Studies. *Anal. Chem.* **2016**, *88* (17), 8802–8811.  
53 415  
54 415 <https://doi.org/10.1021/acs.analchem.6b02222>.
- 55 416 (26) Ji, H.; Zhang, Z.; Lu, H. TarMet: A Reactive GUI Tool for Efficient and  
56 417  
57 417 Confident Quantification of MS Based Targeted Metabolic and Stable Isotope  
58 418  
59 418 Tracer Analysis. *Metabolomics* **2018**, *14* (5), 68. [https://doi.org/10.1007/s11306-](https://doi.org/10.1007/s11306-018-1363-7)  
60 419  
60 419 018-1363-7.

- 1  
2  
3 420 (27) Wills, J.; Edwards-Hicks, J.; Finch, A. J. AssayR: A Simple Mass Spectrometry  
4 Software Tool for Targeted Metabolic and Stable Isotope Tracer Analyses. *Anal.*  
5 421 *Chem.* **2017**, *89* (18), 9616–9619. <https://doi.org/10.1021/acs.analchem.7b02401>.  
6 422  
7  
8 423 (28) Wei, X.; Shi, B.; Koo, I.; Yin, X.; Lorkiewicz, P.; Suhail, H.; Rattan, R.; Giri, S.;  
9 McClain, C. J.; Zhang, X. Analysis of Stable Isotope Assisted Metabolomics  
10 424 Data Acquired by GC-MS. *Anal. Chim. Acta* **2017**, *980*, 25–32.  
11 425  
12 426 <https://doi.org/10.1016/j.aca.2017.05.002>.  
13  
14 427 (29) Ferrazza, R.; Griffin, J. L.; Guella, G.; Franceschi, P. IsotopicLabeling: An R  
15 428 Package for the Analysis of MS Isotopic Patterns of Labeled Analytes.  
16  
17 429 *Bioinformatics* **2017**, *33* (2), 300–302.  
18  
19 430 <https://doi.org/10.1093/bioinformatics/btw588>.  
20  
21 431 (30) Dagley, M. J.; McConville, M. J. DExSI: A New Tool for the Rapid Quantitation  
22 432 of <sup>13</sup>C-Labeled Metabolites Detected by GC-MS. *Bioinformatics* **2018**, *34* (11),  
23 433 1957–1958. <https://doi.org/10.1093/bioinformatics/bty025>.  
24  
25 434 (31) Mairinger, T.; Sanderson, J.; Hann, S. GC–QTOFMS with a Low-Energy  
26 435 Electron Ionization Source for Advancing Isotopologue Analysis in <sup>13</sup>C-Based  
27 436 Metabolic Flux Analysis. *Anal. Bioanal. Chem.* **2019**, *411* (8), 1495–1502.  
28 437  
29 <https://doi.org/10.1007/s00216-019-01590-y>.  
30  
31 438 (32) Selivanov, V. A.; Benito, A.; Miranda, A.; Aguilar, E.; Polat, I. H.; Centelles, J.  
32 439 J.; Jayaraman, A.; Lee, P. W. N.; Marin, S.; Cascante, M. MIDcor, an R-Program  
33 440 for Deciphering Mass Interferences in Mass Spectra of Metabolites Enriched in  
34 441 Stable Isotopes. *BMC Bioinformatics* **2017**, *18* (1), 88.  
35 442  
36 <https://doi.org/10.1186/s12859-017-1513-3>.  
37  
38 443 (33) de Mas, I. M.; Selivanov, V. A.; Marin, S.; Roca, J.; Orešič, M.; Agius, L.;  
39 444 Cascante, M. Compartmentation of Glycogen Metabolism Revealed from <sup>13</sup>C  
40 445 Isotopologue Distributions. *BMC Syst. Biol.* **2011**, *5*, 175.  
41 446  
42 <https://doi.org/10.1186/1752-0509-5-175>.  
43  
44 447 (34) Kalderon, B.; Korman, S. H.; Gutman, A.; Lapidot, A. Glucose Recycling and  
45 448 Production in Glycogenesis Type I and III: Stable Isotope Technique Study. *Am.*  
46 449 *J. Physiol. Metab.* **1989**, *257* (3), E346–E353.  
47 450  
48 <https://doi.org/10.1152/ajpendo.1989.257.3.E346>.  
49  
50 451 (35) Benito, A.; Polat, I. H.; Noé, V.; Ciudad, C. J.; Marin, S.; Cascante, M.; Benito,  
51 452 A.; Polat, I. H.; Noé, V.; Ciudad, C. J.; Marin, S.; Cascante, M.; Benito, A.;  
52 453 Polat, I. H.; Noé, V.; Ciudad, C. J.; Marin, S.; Cascante, M. Glucose-6-Phosphate

- 1  
2  
3 454 Dehydrogenase and Transketolase Modulate Breast Cancer Cell Metabolic  
4  
5 455 Reprogramming and Correlate with Poor Patient Outcome. *Oncotarget* **2017**, *8*  
6  
7 456 (63), 106693–106706. <https://doi.org/10.18632/oncotarget.21601>.  
8  
9 457 (36) Schricker, T.; Albuszies, G.; Kugler, B.; Wachter, U.; Georgieff, M.  
10 458 Determination of Glycerol Turnover by Stable-Isotope Technique in Humans: A  
11  
12 459 New [1,1,2,3,3-2H5]Glycerol Derivative for Mass-Spectrometry Analysis.  
13  
14 460 *Nutrition* *10* (4), 342–345.  
15 461 (37) Mairinger, T.; Steiger, M.; Nocon, J.; Mattanovich, D.; Koellensperger, G.;  
16  
17 462 Hann, S. Gas Chromatography-Quadrupole Time-of-Flight Mass Spectrometry-  
18  
19 463 Based Determination of Isotopologue and Tandem Mass Isotopomer Fractions of  
20  
21 464 Primary Metabolites for <sup>13</sup>C-Metabolic Flux Analysis. *Anal. Chem.* **2015**, *87*  
22  
23 465 (23), 11792–11802. <https://doi.org/10.1021/acs.analchem.5b03173>.  
24 466 (38) Bueno, M. J.; Jimenez-Renard, V.; Samino, S.; Capellades, J.; Junza, A.; López-  
25  
26 467 Rodríguez, M. L.; Garcia-Carceles, J.; Lopez-Fabuel, I.; Bolaños, J. P.; Chandel,  
27  
28 468 N. S.; Yanes, O.; Colomer, R.; Quintela-Fandino, M. Essentiality of Fatty Acid  
29  
30 469 Synthase in the 2D to Anchorage-Independent Growth Transition in  
31  
32 470 Transforming Cells. *Nat. Commun.* **2019**, *10* (1), 5011.  
33  
34 471 <https://doi.org/10.1038/s41467-019-13028-1>.  
35 472 (39) Brunner, J. S.; Vulliard, L.; Hofmann, M.; Kieler, M.; Lercher, A.; Vogel, A.;  
36  
37 473 Russier, M.; Brüggenthies, J. B.; Kerndl, M.; Saferding, V.; Niederreiter, B.;  
38  
39 474 Junza, A.; Frauenstein, A.; Scholtysek, C.; Mikami, Y.; Klavins, K.; Krönke, G.;  
40  
41 475 Bergthaler, A.; O'Shea, J. J.; Weichhart, T.; Meissner, F.; Smolen, J. S.; Cheng,  
42  
43 476 P.; Yanes, O.; Menche, J.; Murray, P. J.; Sharif, O.; Blüml, S.; Schabbauer, G.  
44  
45 477 Environmental Arginine Controls Multinuclear Giant Cell Metabolism and  
46  
47 478 Formation. *Nat. Commun.* **2020**, *11* (1), 1090. [https://doi.org/10.1038/s41467-](https://doi.org/10.1038/s41467-020-14285-1)  
48  
49 479 020-14285-1.  
50 480 (40) Llinàs-Arias, P.; Rosselló-Tortella, M.; López-Serra, P.; Pérez-Salvia, M.; Setién,  
51  
52 481 F.; Marin, S.; Muñoz, J. P.; Junza, A.; Capellades, J.; Calleja-Cervantes, M. E.;  
53  
54 482 Ferreira, H. J.; Moura, M. C. de; Srbic, M.; Martínez-Cardús, A.; Torre, C. de la;  
55  
56 483 Villanueva, A.; Cascante, M.; Yanes, O.; Zorzano, A.; Moutinho, C.; Esteller, M.  
57  
58 484 Epigenetic Loss of the Endoplasmic Reticulum–Associated Degradation Inhibitor  
59  
60 485 SVIP Induces Cancer Cell Metabolic Reprogramming. *JCI Insight* **2019**, *4* (8).  
61  
62 486 <https://doi.org/10.1172/JCI.INSIGHT.125888>.  
63  
64 487 (41) Cano-Crespo, S.; Chillarón, J.; Junza, A.; Fernández-Miranda, G.; García, J.;

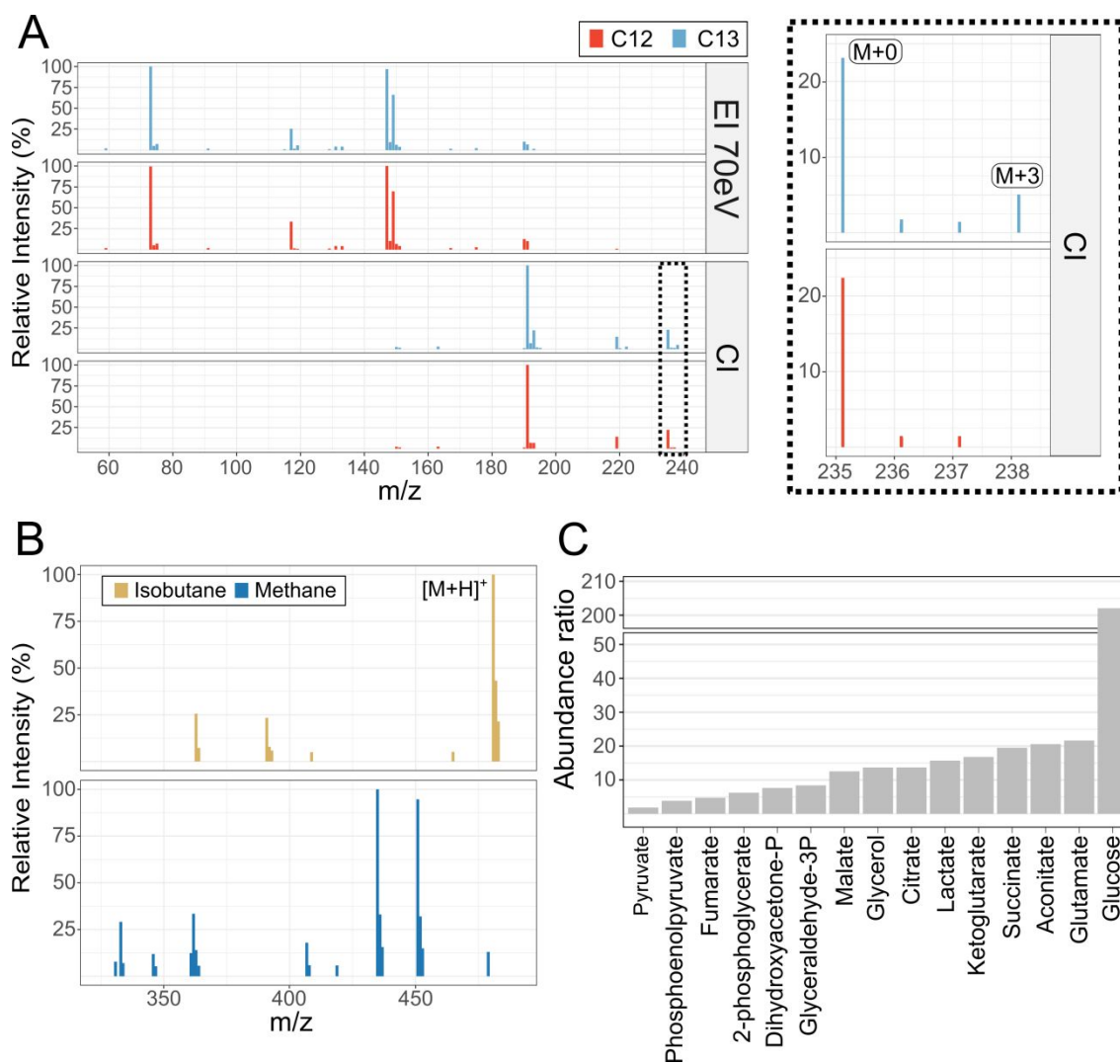
- 1  
2  
3 488 Polte, C.; R. de la Ballina, L.; Ignatova, Z.; Yanes, Ó.; Zorzano, A.; Stephan-Otto  
4 489 Attolini, C.; Palacín, M. CD98hc (SLC3A2) Sustains Amino Acid and  
5 490 Nucleotide Availability for Cell Cycle Progression. *Sci. Rep.* **2019**, *9* (1), 14065.  
6 491 <https://doi.org/10.1038/s41598-019-50547-9>.  
7  
8  
9  
10 492 (42) Soukupova, J.; Malfettone, A.; Hyroššová, P.; Hernández-Alvarez, M.-I.;  
11 493 Peñuelas-Haro, I.; Bertran, E.; Junza, A.; Capellades, J.; Giannelli, G.; Yanes, O.;  
12 494 Zorzano, A.; Perales, J. C.; Fabregat, I. Role of the Transforming Growth Factor-  
13 495  $\beta$  in Regulating Hepatocellular Carcinoma Oxidative Metabolism. *Sci. Rep.* **2017**,  
14 496 *7* (1), 12486. <https://doi.org/10.1038/s41598-017-12837-y>.  
15  
16  
17 497 (43) Lahiguera, Á.; Hyroššová, P.; Figueras, A.; Garzón, D.; Moreno, R.;  
18 498 Soto-Cerrato, V.; McNeish, I.; Serra, V.; Lazaro, C.; Barretina, P.; Brunet, J.;  
19 499 Menéndez, J.; Matias-Guiu, X.; Vidal, A.; Villanueva, A.; Taylor-Harding, B.;  
20 500 Tanaka, H.; Orsulic, S.; Junza, A.; Yanes, O.; Muñoz-Pinedo, C.; Palomero, L.;  
21 501 Pujana, M. À.; Perales, J. C.; Viñals, F. Tumors Defective in Homologous  
22 502 Recombination Rely on Oxidative Metabolism: Relevance to Treatments with  
23 503 PARP Inhibitors. *EMBO Mol. Med.* **2020**.  
24 504 <https://doi.org/10.15252/emmm.201911217>.  
25  
26  
27 505 (44) Loos, M.; Gerber, C.; Corona, F.; Hollender, J.; Singer, H. Accelerated Isotope  
28 506 Fine Structure Calculation Using Pruned Transition Trees. *Anal. Chem.* **2015**, *87*  
29 507 (11), 5738–5744. <https://doi.org/10.1021/acs.analchem.5b00941>.  
30  
31  
32 508 (45) Newsome, G. A.; Steinkamp, F. L.; Giordano, B. C. Isobutane Made Practical as  
33 509 a Reagent Gas for Chemical Ionization Mass Spectrometry. *J. Am. Soc. Mass*  
34 510 *Spectrom.* **2016**, *27* (11), 1789–1795. [https://doi.org/10.1007/s13361-016-1463-](https://doi.org/10.1007/s13361-016-1463-4)  
35 511 [4](https://doi.org/10.1007/s13361-016-1463-4).  
36  
37  
38  
39  
40  
41  
42  
43  
44  
45  
46  
47  
48  
49  
50  
51  
52  
53  
54  
55  
56  
57  
58  
59  
60

1  
2  
3 515 For Table of Contents Only  
4  
5



516

517



518

519

520

521

522

523

524

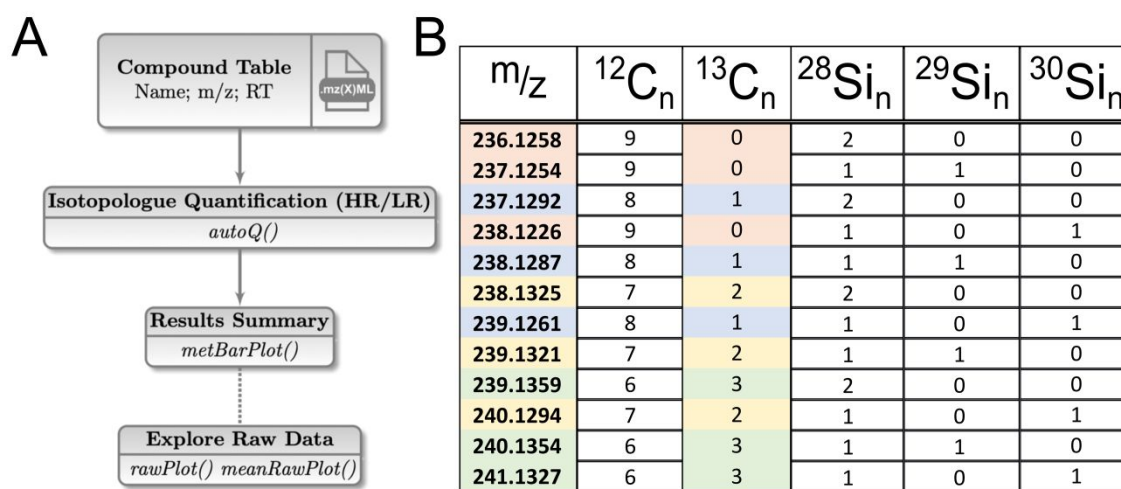
525

526

**Figure 1. Comparison of EI and CI.** (A) Lactate 2TMS spectra obtained from non-labeled (red) and <sup>13</sup>C<sub>6</sub>-Glucose labeled (blue) cell cultures. Top spectra show electron impact ionization mass spectral fragments of lactate. Bottom spectra show ions produced by chemical ionization, where the isotopic envelope of intact [M+H]<sup>+</sup> ion is squared and zoomed in. (B) Chemical ionization spectra of Citrate 4TMS using isobutane and methane as reagent gases. (C) Protonated [M+H]<sup>+</sup> ion abundance ratios (isobutane/methane) of glycolysis and TCA cycle compounds.



1  
2  
3 536 a QqQ mass analyzer (n=9). (C) Relative deviation of isotopologue abundances in  
4  
5 537 relation to theoretical natural abundances, experimentally calculated from 8 and 23  
6  
7 538 metabolites, using TOF and Orbitrap mass analyzers, respectively (n=5-10). Blue  
8  
9 539 shade indicates the range of relative theoretical abundance per ion. (D) Relative  
10  
11 540 abundances of isotopologue ions of lactate 2TMS, malate 3TMS, aconitate 3TMS  
12  
13 541 and dihydroxy-acetone phosphate 3TMS+methoxyamine (MA) from NS acquisition  
14  
15 542 using a QqQ mass analyzer, and full scan using an Orbitrap mass analyzer. In these,  
16  
17 543 the spectra belong to a  $^{13}\text{C}$ -labeled sample.  
18  
19  
20  
21  
22  
23  
24  
25  
26  
27  
28  
29  
30  
31  
32  
33  
34  
35  
36  
37  
38  
39  
40  
41  
42  
43  
44  
45  
46  
47  
48  
49  
50  
51  
52  
53  
54  
55  
56  
57  
58  
59  
60



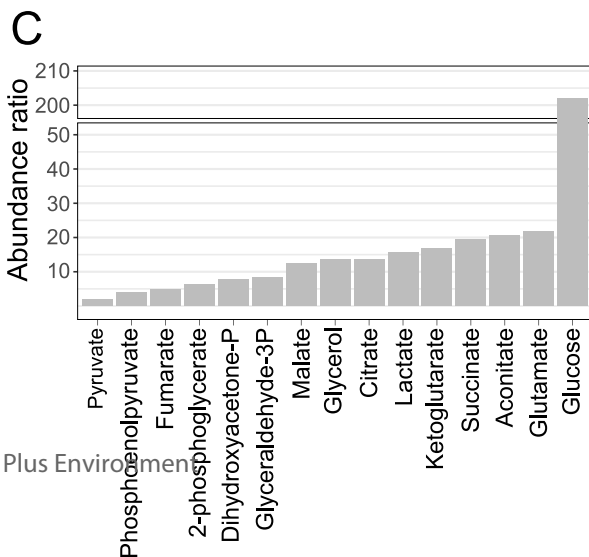
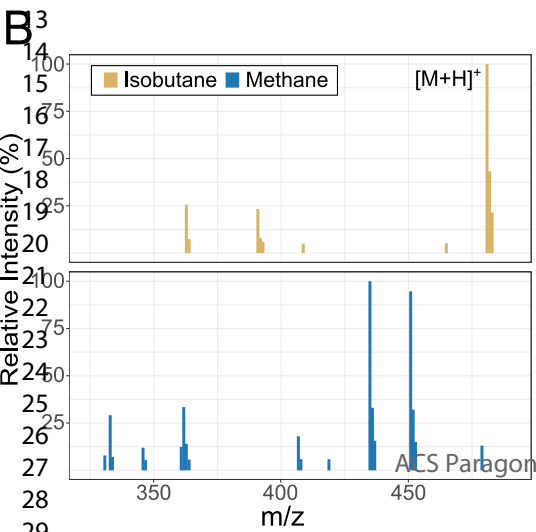
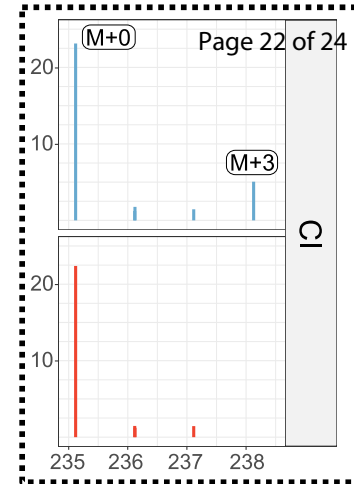
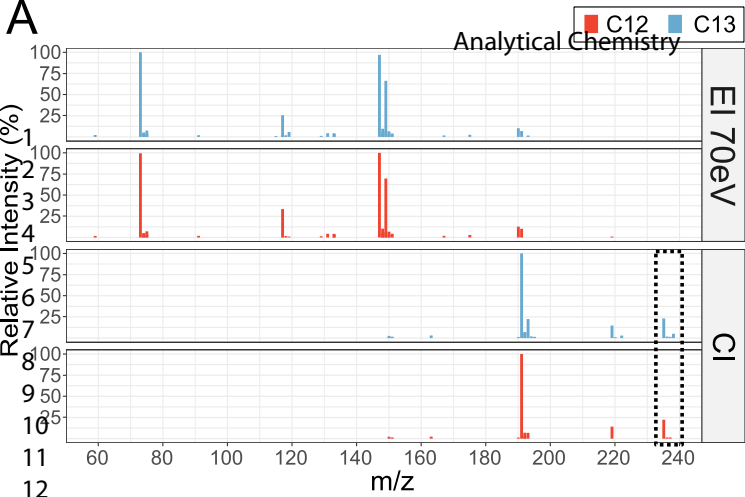
545

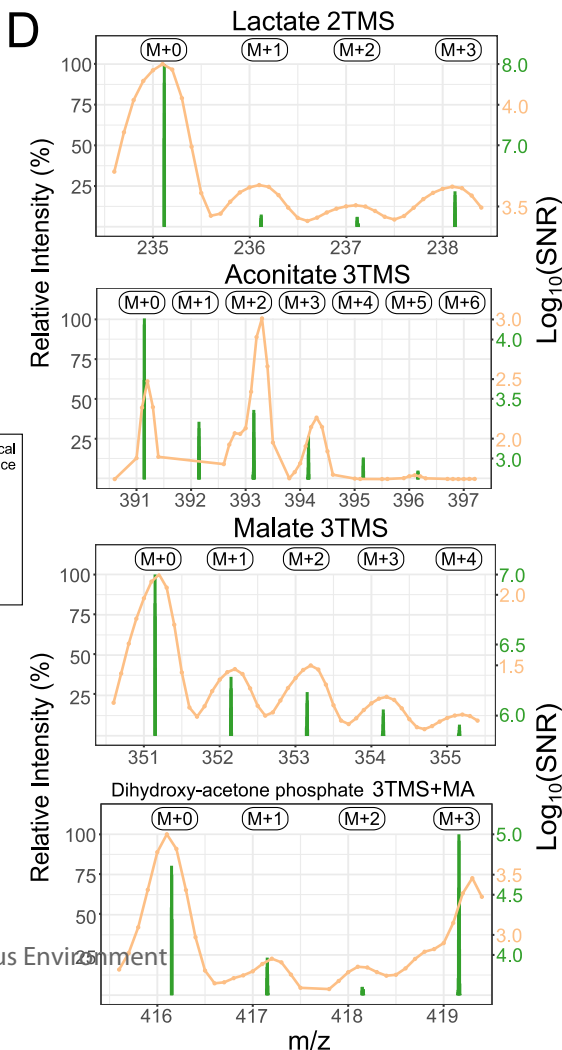
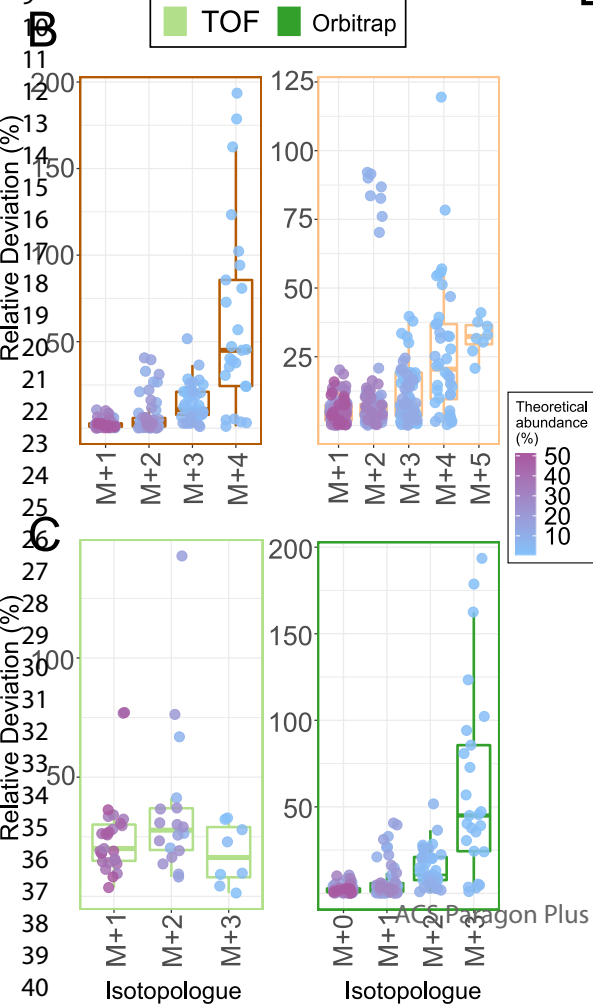
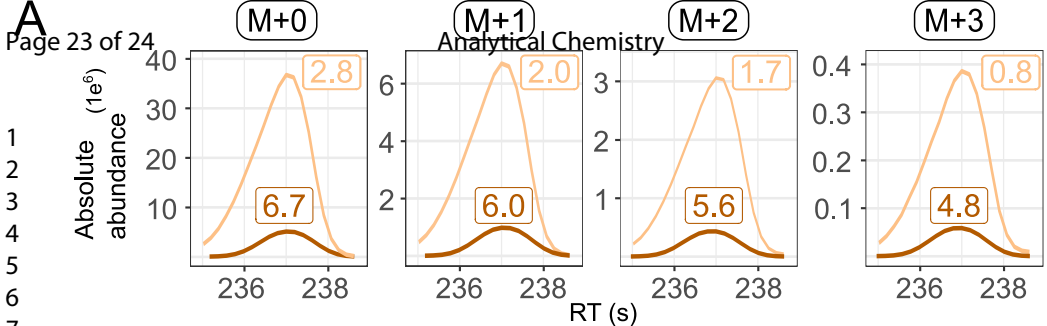
546

547

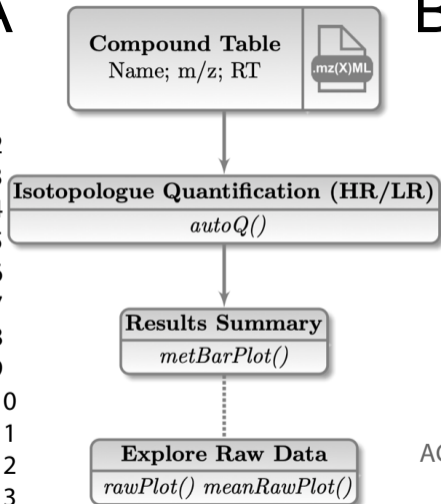
548 **Figure 3. Data input and function hierarchy of isoSCAN.** A) isoSCAN R-  
 549 package main workflow: *autoQ* function performs quantification for both low  
 550 (LR) and high-resolution (HR) data. The input of *autoQ* is a list of targeted  
 551 compounds and mz(X)ML files, and its results can be plotted using *metBarPlot*.  
 552 In addition, raw data can be explored by separate functions. B) Isotopologues to  
 553 consider in HRMS for Lactate 2TMS ( $\text{C}_9\text{H}_{24}\text{O}_3\text{Si}_2$ ). Each color determines ions  
 554 that should be summed for correct isotopologue estimation if  $^{13}\text{C}$  enrichment is to  
 555 be quantified.

555





A

1  
2  
3  
4  
5  
6  
7  
8  
9  
10  
11  
12  
13  
14

B

Analytical Chemistry Page 24 of 24

m/z	<sup>12</sup> C <sub>n</sub>	<sup>13</sup> C <sub>n</sub>	<sup>28</sup> Si <sub>n</sub>	<sup>29</sup> Si <sub>n</sub>	<sup>30</sup> Si <sub>n</sub>
236.1258	9	0	2	0	0
237.1254	9	0	1	1	0
237.1292	8	1	2	0	0
238.1226	9	0	1	0	1
238.1287	8	1	1	1	0
238.1325	7	2	2	0	0
239.1261	8	1	1	0	1
239.1321	7	2	1	1	0
239.1359	6	3	2	0	0
240.1294	7	2	1	0	1
240.1354	6	3	1	1	0
241.1327	6	3	1	0	1

ACS Paragon Plus Environment